Novel MIMO Antenna System for Ultra Wideband Applications

Abdullah G. Alharbi [1], Umair Rafique [2,*], Shakir Ullah [3], Salahuddin Khan [4], Syed Muzahir Abbas [5], Esraa Mousa Ali [6], Mohammad Alibakhshikenari [7] and Mariana Dalarsson [8,*]

[1] Department of Electrical Engineering, Faculty of Engineering, Jouf University, Sakaka 42421, Saudi Arabia; a.g.alharbi@ieee.org
[2] Department of Information Engineering, Electronics, and Telecommunications, Sapienza University of Rome, 00184 Rome, Italy
[3] Telecommunication Engineering Department, University of Engineering & Technology, Mardan 23200, Pakistan; shakirhayat.eng@gmail.com
[4] College of Engineering, King Saud University, P.O. Box 800, Riyadh 11421, Saudi Arabia; drskhan@ksu.edu.sa
[5] Faculty of Science and Engineering, School of Engineering, Macquarie University, Sydney, NSW 2109, Australia; syed.abbas@mq.edu.au
[6] Faculty of Aviation Sciences, Amman Arab University, Amman 11953, Jordan; esraa_ali@aau.edu.jo
[7] Department of Signal Theory and Communications, Universidad Carlos III de Madrid, 28911 Leganés, Madrid, Spain; mohammad.alibakhshikenari@uc3m.es
[8] School of Electrical Engineering and Computer Science, KTH Royal Institute of Technology, SE 100-44 Stockholm, Sweden
* Correspondence: umair.rafique@uniroma1.it (U.R.); mardal@kth.se (M.D.)

Abstract: The design of a 4 × 4 MIMO antenna for UWB communication systems is presented in this study. The single antenna element is comprised of a fractal circular ring structure backed by a modified partial ground plane having dimensions of 30 × 30 mm^2. The single antenna element has a wide impedance bandwidth of 9.33 GHz and operates from 2.67 GHz to 12 GHz. Furthermore, the gain of a single antenna element increases as the frequency increases, with a peak realized gain and antenna efficiency of 5 dBi and >75%, respectively. For MIMO applications, a 4 × 4 array is designed and analyzed. The antenna elements are positioned in a plus-shaped configuration to provide pattern as well as polarization diversity. It is worth mentioning that good isolation characteristics are achieved without the utilization of any isolation enhancement network. The proposed MIMO antenna was fabricated and tested, and the results show that it provides UWB response from 2.77 GHz to over 12 GHz. The isolation between the antenna elements is more than 15 dB. Based on performance attributes, it can be said that the proposed design is suitable for UWB MIMO applications.

Keywords: 4 × 4 MIMO; UWB communication; fractal circular ring; pattern and polarization diversity; plus shape configuration

1. Introduction

Recent progress in wireless communication necessitates a system capable of sharing massive amounts of data quickly with increased capacity, dependability, and security with less complexity. Ultra wideband (UWB) technology can meet these expectations since it allows high data rates while employing low-cost infrastructure [1,2]. The traditional UWB technology, on the other hand, has problems with multipath propagation. To mitigate this effect, multiple-input multiple-output (MIMO) technology has been introduced. Furthermore, one of the most promising solutions for meeting the needs of UWB systems is to design MIMO antennas. It is a difficult task to design such an antenna because it adds extra performance characteristics to consider. Antenna element isolation is one of the most essential performance characteristics, which should be as low as possible to avoid channel capacity loss.

Several configurations for improving isolation have been published in the literature. Designing stubs with the ground plane or the radiating element helps improve isolation

between MIMO antenna elements. In [3], a spatial diversity-based MIMO antenna was designed for UWB applications. To obtain a wide impedance bandwidth, a triangular-shaped patch radiator with a modified ground plane was used. The radiators do not radiate directly towards each other, which can lead to better isolation. In the ground plane, inverted L-shaped stubs and a complementary split ring resonance (CSRR) were designed to improve isolation even further. The authors in [4] utilized the same kind of configuration. In this design, a tapered fed polygon-shaped patch radiator was designed to achieve UWB response. The authors in [5] used the same type of isolation enhancement technique as presented in [3,4]. They designed a co-planar waveguide (CPW)-fed beveled-shaped patch radiator to achieve a UWB response. In addition, the radiating structure was composed of two half-wavelength rectangular single CSRRs (RSCSRRs) of different dimensions to achieve band notch characteristics for Worldwide Interoperability for Microwave Access (WiMAX) and Wireless Local Area Network (WLAN) frequency bands. In [6], an eye-shaped slot radiator-based MIMO antenna design was presented. The ground plane was developed with an extruded T-shaped stub to improve isolation. This simple configuration tends to achieve an isolation of >20 dB and ECC < 0.02. In [7], a 2-element dual-ring-based MIMO antenna was designed. The main patch radiator consists of a ring element, while the second ring behaves as a parasitic element. To improve the isolation between the antennas, two inverted U-stubs were designed into the ground plane.

The employment of electromagnetic bandgap (EBG) structures, metamaterials, and frequency-selective surfaces (FSSs) to increase MIMO antenna element isolation has been proposed in the literature as a viable technology. In [8], a modified radiator with a FSS was reported. The design was non-planar, with four elements placed around a cube of polystyrene. A quad-port cognitive radio MIMO antenna was presented in [9]. The single antenna consists of a circular monopole geometry and a $\lambda/4$ monopole for the notch band. For high isolation, multiple EBG cells having different dimensions and an isolating stub between the UWB and notch band radiators were employed. A two-port MIMO antenna with improved E-plane isolation was presented in [10]. A meandered EBG structure was designed on both sides of the substrate to improve isolation. In [11], a MIMO antenna design was presented having arrow shaped radiator. The presented design operates within the UWB spectrum with three notch bands obtained by cutting the slots within the radiator. To improve the isolation performance, a T-shaped stub was used with the ground plane, and two EBG cells were placed on each side of the feeding line. Additionally, the size of the structure is quite large for a two-port configuration. In [12], a miniaturized UWB MIMO antenna design was presented. The MIMO antenna elements were composed of a combination of rectangle and semi-circular arc fed using a stepped microstrip fee line. For improved isolation between MIMO elements, a Jerusalem cross-shaped FSS structure and a meandered-shaped decoupling structure were designed. All the above-reported designs have EBG/FSS structures, which are complex to fabricate as they have a "via" that connects the top and ground plane and are large in size.

The use of neutralization lines or decoupling structures between the radiators can also provide high isolation. In [13], a decoupling strip was diagonally placed between the antenna elements for isolation enhancement. In addition, a dumbbell-shaped stub was designed with the ground plane, and the same was placed on the top side of the substrate. From the presented configuration, an isolation of >15 dB was achieved in the frequency range of 3–11 GHz. In [14], a four-port dual-band nocth UWB MIMO antenna was presented. Four rhombic-shaped patch radiators were arranged in a polarization diversity configuration. Two CSRRs were etched from the radiators to reject WLAN and WiMAX frequency bands. A plus-shaped metal strip was designed with the ground plane for enhanced isolation. In [15], a design for a compact super wideband (SWB) antenna was presented. The presented SWB radiator geometry consists of a combination of circular, rectangular, and trapezoidal shapes. The bandwidth of the antenna was enhanced by placing slots in the radiator and by a modified ground plane. Different MIMO configurations were analyzed, such as spatial, pattern, and polarization diversity with a common

ground plane. From the presented configurations, an isolation of ≥30 dB was achieved. In [16], an octagonal band notch UWB MIMO antenna design was demonstrated. Two hexagonal-shaped CSRRs (HCSRRs) were etched from the octagonal radiator to achieve band stop characteristics around the WLAN and WiMAX frequency bands. A decoupling structure consisting of three thin metal strips was designed in the middle of the radiation elements to achieve an isolation of >18 dB in the UWB frequency range. The same kind of isolation enhancement technique was described in [17]. In [18], a simple polarization diversity-based four-element MIMO configuration was presented for UWB applications. The single antenna element consists of a combination of rectangular and circular patch radiators. In [19], an eight-element semi-circular arc-based MIMO antenna design was presented for UWB applications. The UWB response was achieved by etching a semi-elliptical slot in the ground plane and designing an inverted L-shaped strip in conjunction with the ground plane. Initially, the authors realized a four-element MIMO antenna design placed in a plus-shaped configuration. After that, an eight-element MIMO antenna configuration was demonstrated for UWB applications. Thin metallic strips were designed between the radiators to achieve an isolation of >15 dB in the frequency range of 2.84–11 GHz.

In the literature, some researchers utilized defected ground structures (DGSs) to improve the isolation between MIMO antennas. A two-element aperture-coupled complementary Sierpinski gasket equilateral triangular fractal MIMO antenna was designed for UWB performance in [20]. For enhanced isolation, a complementary Archimedean spiral-based DGS was utilized. The use of DGS led to an isolation level of ≥15.8 dB. In [21], for UWB applications, a MIMO antenna with good isolation was demonstrated. For MIMO antenna design, slot elements having quasi F-shaped radiators and L-shaped open-slots were adopted. In the ground plane, a decoupling structure consisting of a thin slot and a fork-shaped slot was implemented to increase isolation between the radiators and in the lower band.

The techniques presented above provide better isolation between antenna elements, but they are quite complex and their fabrication is difficult. In this paper, a novel MIMO antenna configuration is presented for UWB applications. The antenna elements are positioned in a plus-shaped arrangement to provide pattern and polarization diversity [19,22]. It is observed from the presented results that the designed MIMO antenna operates from 2.77–12 GHz. Furthermore, the presented MIMO antenna did not utilize any isolation enhancement technique, which makes it simple and it can easily be fabricated through low-cost fabrication techniques.

2. Proposed MIMO Configuration

2.1. Mimo Single Element

The design of a single antenna element is depicted in Figure 1. The front side of the designed antenna consists of a fractal circular ring radiator [23] fed using a 50 Ω microstrip feed line (see Figure 1a), while the back side consists of a notch loaded trapezoidal partial ground plane, as illustrated in Figure 1b. The radius R_1 of the outer circular ring is calculated using the design expressions mentioned in [24], and the width of the feeding line is calculated using the procedure described in [25]. From Figure 1a, one can observe that six circular rings of radius R_3 are embedded in the main radiator to realize a fractal geometry. These rings are rotated at an angle of 60°. Furthermore, the trapezoidal ground plane is utilized (see Figure 1b) to create wideband multi-resonance characteristics of the input impedance, which leads to achieving enhanced bandwidth [26], while the square notch etched from the ground plane offers maximum impedance matching in the operating bandwidth. The proposed antenna is designed using a low-cost FR-4 laminate with $\epsilon_r = 4.3$ and $h = 1.6$ mm. The overall design dimensions of the antenna are: $W_S = 30$, $L_S = 30$, $R_1 = 9.5$, $R_2 = 7.5$, $R_3 = 3.5$, $R_4 = 2.4$, $W_f = 3$, $L_f = 10$, $W_g = 30$, $L_g = 9.5$, $L_{g1} = 5.5$, and $S = 3$ (all dimensions are in mm).
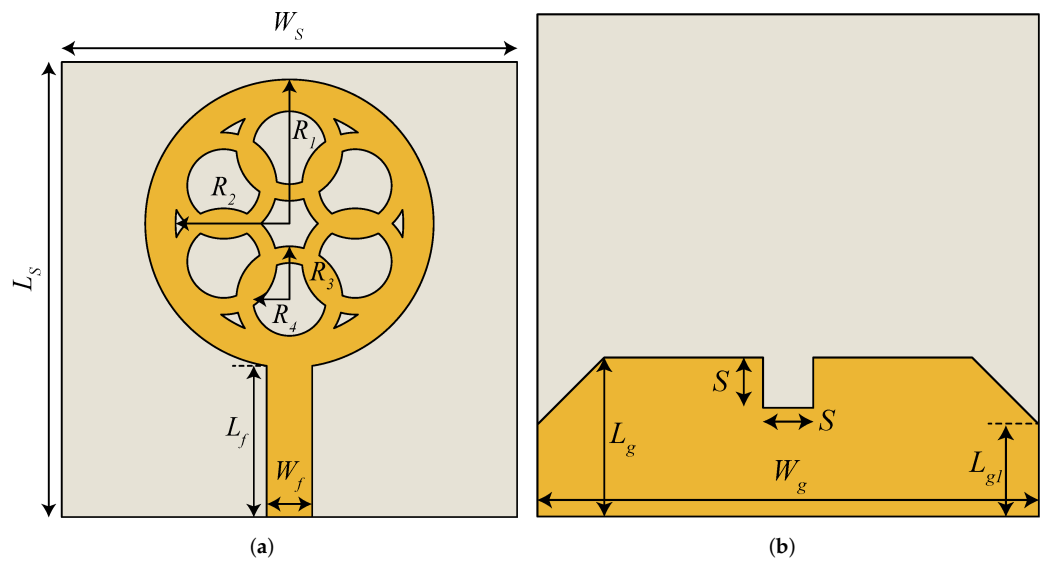
Figure 1. Schematic of the proposed single antenna element (**a**) front side (**b**) back side.

The construction of the proposed antenna starts with the design of a circular ring patch radiator backed by a conventional partial ground plane, shown in Figure 2a, and its respective reflection coefficient (S$_{11}$) is depicted in Figure 3. From the results, it is observed that the circular ring provides a dual-band response around 3 GHz and 10 GHz. To excite more resonant modes in the band of interest, six circular rings of radius R_3 are embedded in the main radiator (see Figure 2b), which ultimately leads to a fractal geometry. This configuration increased the impedance bandwidth, but there is still a mismatch between 7.58 GHz and 9.38 GHz (see Figure 3). To improve the impedance matching, a trapezoidal shaped ground plane with a square notch is utilized, as shown in Figure 2c. The modification in the ground structure leads to achieving an UWB frequency response ranging from 2.69 GHz to 12 GHz, as shown in Figure 3.
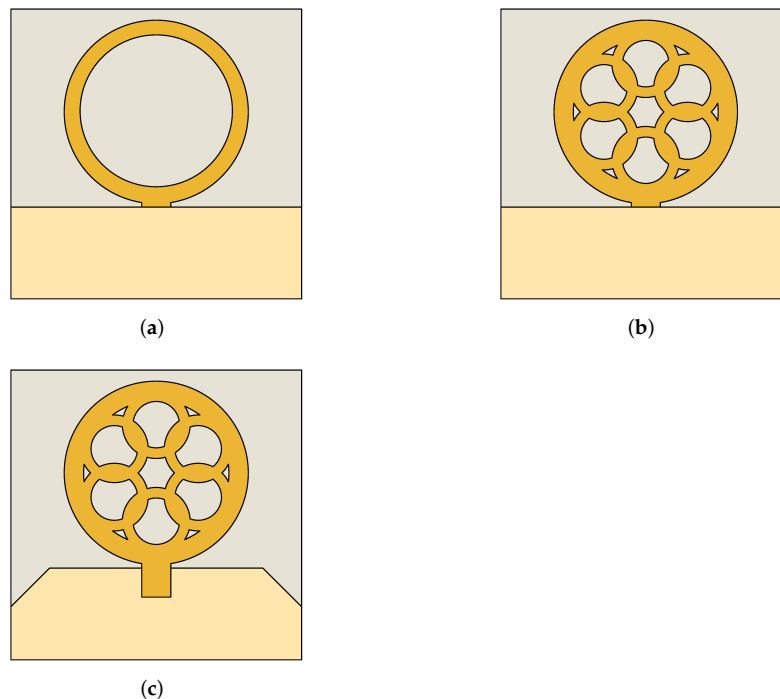
Figure 2. Design evolution of single antenna element. (**a**) Step-1. (**b**) Step-2. (**c**) Step-3 (Proposed).
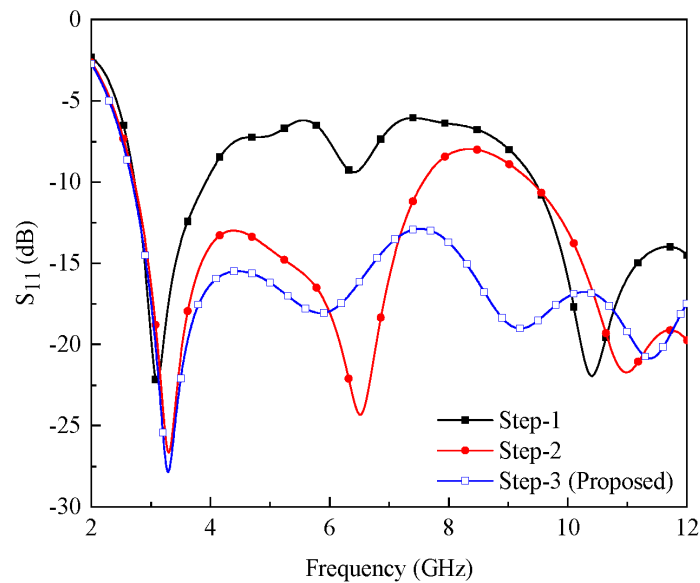
Figure 3. Reflection coefficients (S_{11}) of different design stages.

Figure 4 depicts the presented antenna element's realized gain and radiation efficiency. The antenna gain varies in the range of 0.55–5 dBi in the operating bandwidth, while the radiation efficiency is noted to be >75% in the band of interest (see Figure 4).
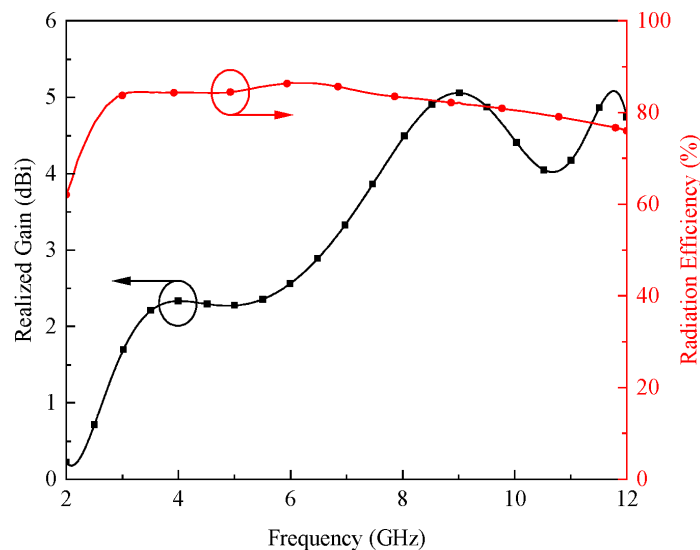
Figure 4. Simulated realized gain and radiation efficiency of single antenna element.

2.2. 4 × 4 MIMO Design

The proposed MIMO antenna configuration is shown in Figure 5. From the figure, one can observe that four antenna elements are arranged in a plus-shaped configuration, which tends to achieve both pattern and polarization diversity. Antenna-1 and antenna-2 are placed at a 90° angle, which is the typical configuration of polarization diversity, while antenna-1 and antenna-3 offer pattern diversity (see Figure 5). As a whole, each antenna element is able to provide both pattern and polarization diversity characteristics. It is also worth mentioning that no decoupling network is used to enhance the isolation between antenna elements. The dimensions of the antenna elements are the same as those of a single element (see Figure 1). As shown in Figure 5a, there is an extra space created between the antenna elements, which is represented by $W_{S1} \times L_{S1} = 30 \times 30$ mm^2. Therefore, the overall dimensions of the proposed MIMO antenna are 90×90 mm^2 (consider both sides of the plus shape).
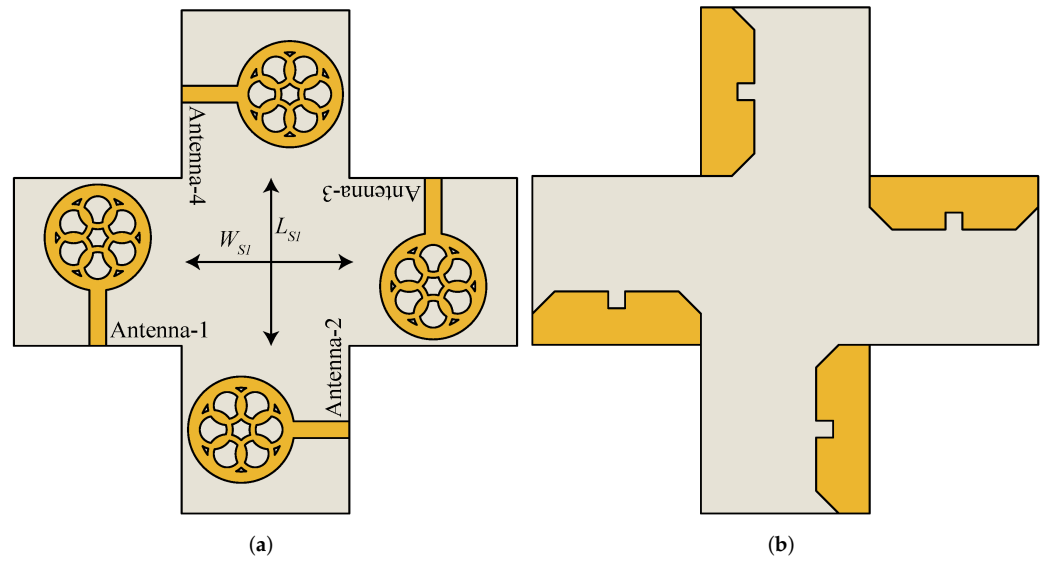
Figure 5. Configuration of the proposed UWB MIMO antenna (**a**) front side (**b**) back side.

Computer Simulation Technology (CST) Microwave Studio 2021 was used to develop and simulate the proposed MIMO antenna. The simulated S-parameters of the designed MIMO are shown in Figure 6. In the figure, the reflection coefficients are represented by S_{ii} ($i \in 1, 2, 3, 4$), while the isolation between adjacent elements is denoted by S_{ji} ($i, j \in 1, 2, 3, 4$ and $i \neq j$), and for parallel elements, it is represented by S_{ki} ($k, i \in 1, 2, 3, 4$ and $|k - i| = 2$). The MIMO antenna's impedance bandwidth is 9.27 GHz in the range of 2.73–12 GHz. Furthermore, the isolation between adjacent antenna elements, denoted by S_{ji}, is >17 dB whereas the isolation between parallel elements, denoted by S_{ki}, is ≥14 dB.

To better understand the isolation characteristics, the surface current distribution (see Figure 7) is plotted by exciting only port-1 of the array, while the rest of the ports are terminated with a 50 Ω matched load. Three different frequencies, such as 3 GHz, 6 GHz, and 9 GHz, are used to depict the surface current. It can be observed from Figure 7 that the surface current generated by antenna-1 does not influence adjacent or parallel placed elements.
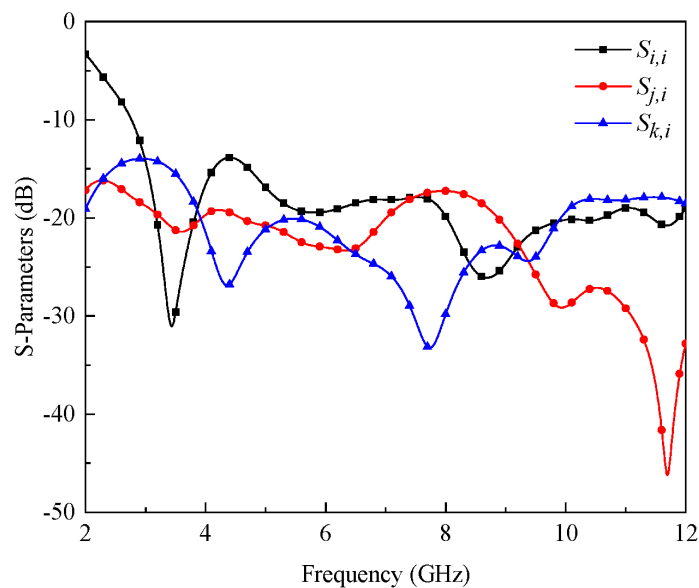
Figure 6. Simulated S-parameters of the proposed UWB MIMO antenna.

(a)

(b)

(c)
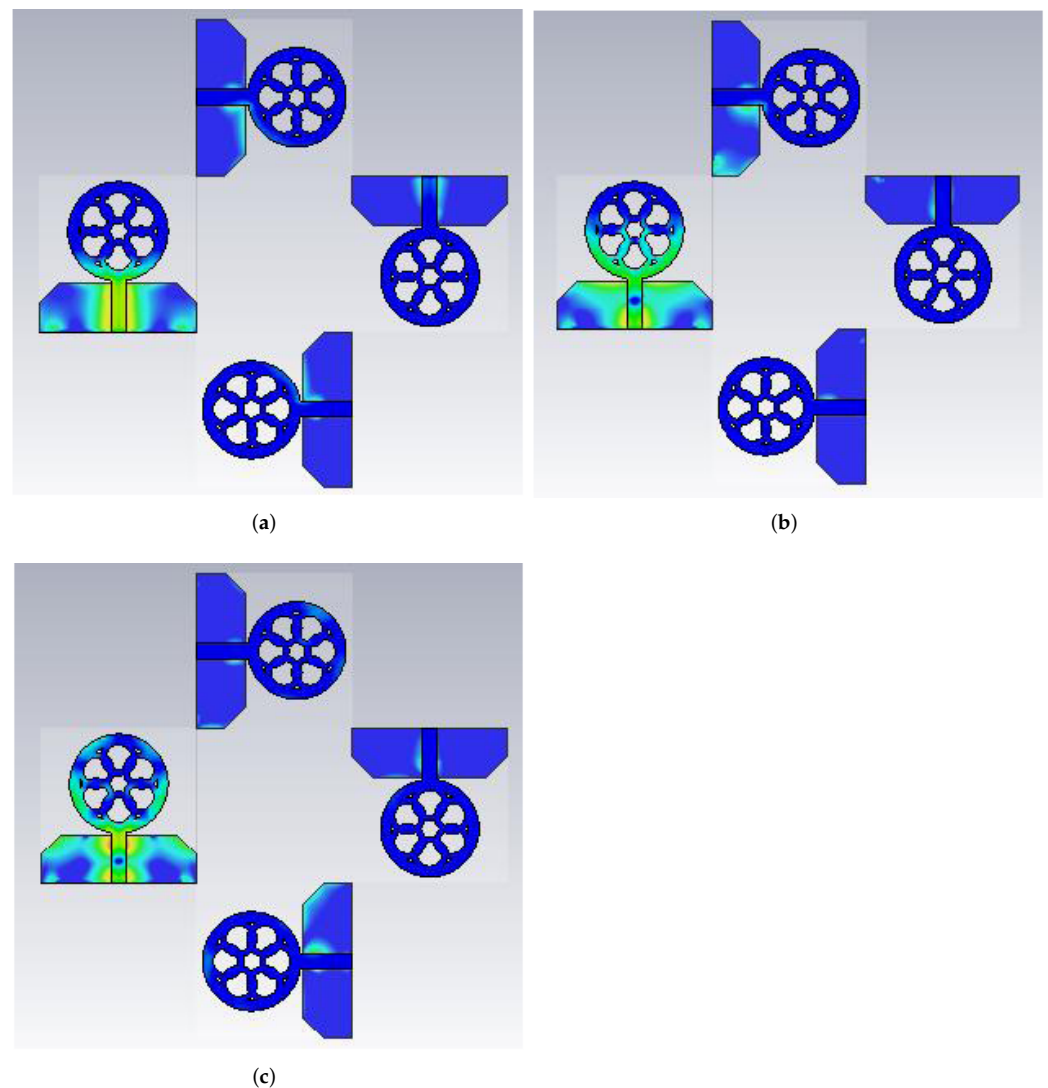
Figure 7. Surface current distribution of the proposed UWB MIMO antenna when port-1 is excited. (**a**) 3 GHz. (**b**) 6 GHz. (**c**) 9 GHz.

3. Fabrication and Measured Results

A prototype of the four-element MIMO antenna was fabricated (see Figure 8) to verify the simulations. For measurement purposes, a Precision Network Analyzer (PNA) E8363C by Agilent Technologies is utilized. The measured S-parameters are shown in Figure 9. Due to symmetry, the reflection coefficients of antenna-1 and antenna-2 are presented. From Figure 9, it is evident that the measured S-parameters matched well with the simulated ones (see Figure 6). The measured impedance bandwidth is 9.23 GHz in the frequency range of 2.77–12 GHz. As demonstrated in Figure 9b, the observed isolation is >15 dB for both neighbouring and parallel antenna elements. The discrepancies between the results are due to SMA connector losses and fabrication intolerances.

Figures 10–13 demonstrate the radiation parameters of the proposed MIMO antenna for all ports at frequencies of 3 GHz, 6 GHz, and 9 GHz. In case of port-1, for 3 GHz (see Figure 10a), omnidirectional pattern is observed for *xz*-plane ($\phi = 0°$), while for *yz*-plane ($\phi = 90°$), antenna exhibits typical monopole like pattern. For 6 GHz, a quasi-omnidirectional pattern is noted for *xz*-plane and a monopole like pattern is observed for *yz*-plane, as shown in Figure 10b. For higher frequencies, such as 9 GHz, a quasi-omnidirectional pattern with some ripples is observed for both the planes, as illustrated in Figure 10c. For port-2, the same kinds of patterns are observed, but in this case, antenna-1

xz-plane radiation pattern is equal to antenna-2's *yz*-plane radiation pattern, and vice versa. This effect can clearly be observed from the patterns in Figure 11. From Figure 12, one can observe that antenna-3 offers the same radiation characteristics as antenna-1. In this case, the *yz*-plane of antenna-3 provides pattern diversity for the reported frequency bands. The same is the case with antenna-4, whose *yz*-plane offers pattern diversity in comparison to antenna-2's characteristics. As a whole, from the results of Figures 10–13, one can observe that all the antenna elements have the ability to exhibit pattern and polarization diversity. Furthermore, from Figures 10–13, one can also observe that the simulated and measured radiation characteristics are in good agreement. Some discrepancies are observed between the simulated and measured data, especially at higher frequencies (9 GHz), which could possibly arise due to fabrication tolerances at higher frequencies and far-field measurement setup losses.

(**a**)　　　　　　　　　　　　　　(**b**)
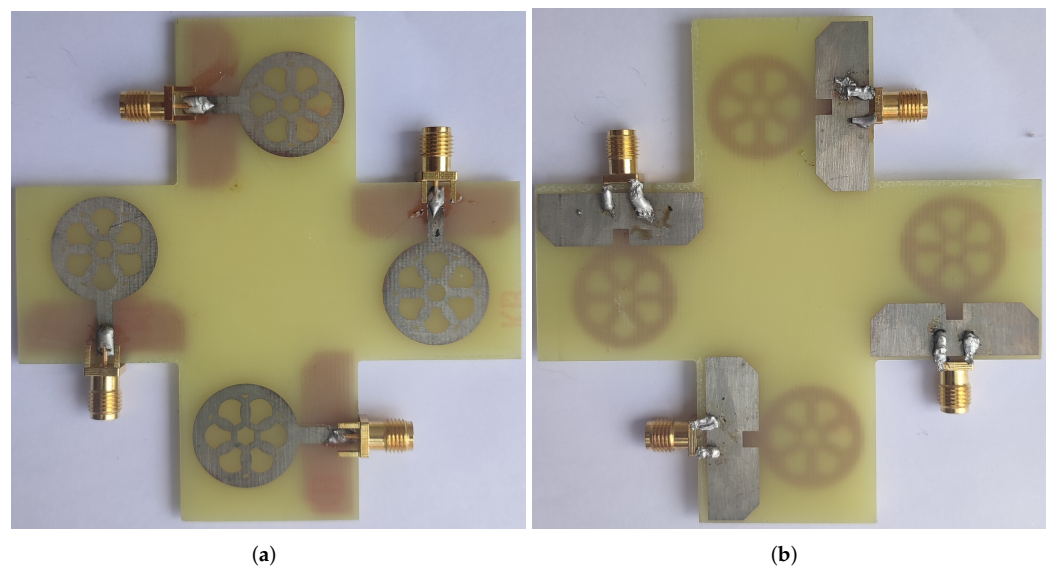
Figure 8. Fabricated prototype of the proposed UWB MIMO antenna (**a**) front side (**b**) back side.

(**a**)　　　　　　　　　　　　　　(**b**)
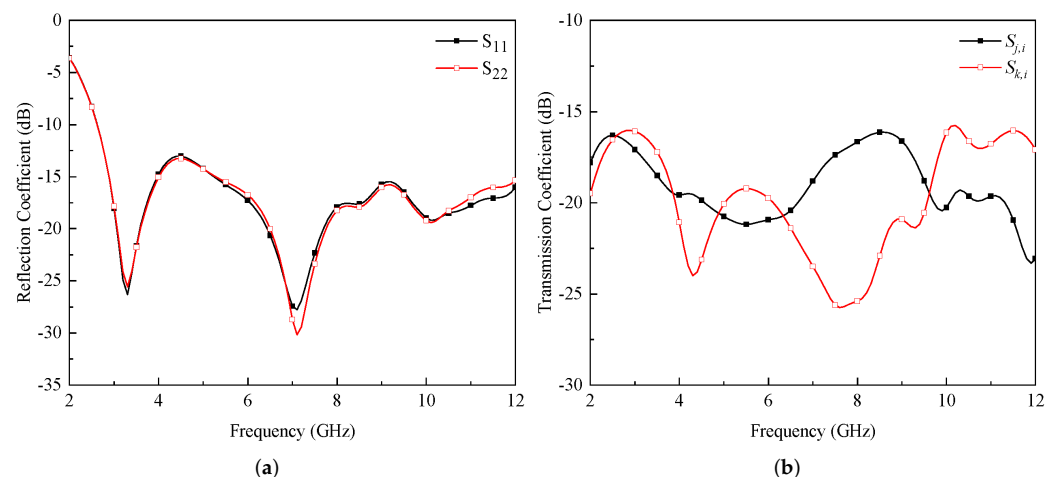
Figure 9. Measured (**a**) reflection and (**b**) transmission coefficients of the proposed UWB MIMO antenna.
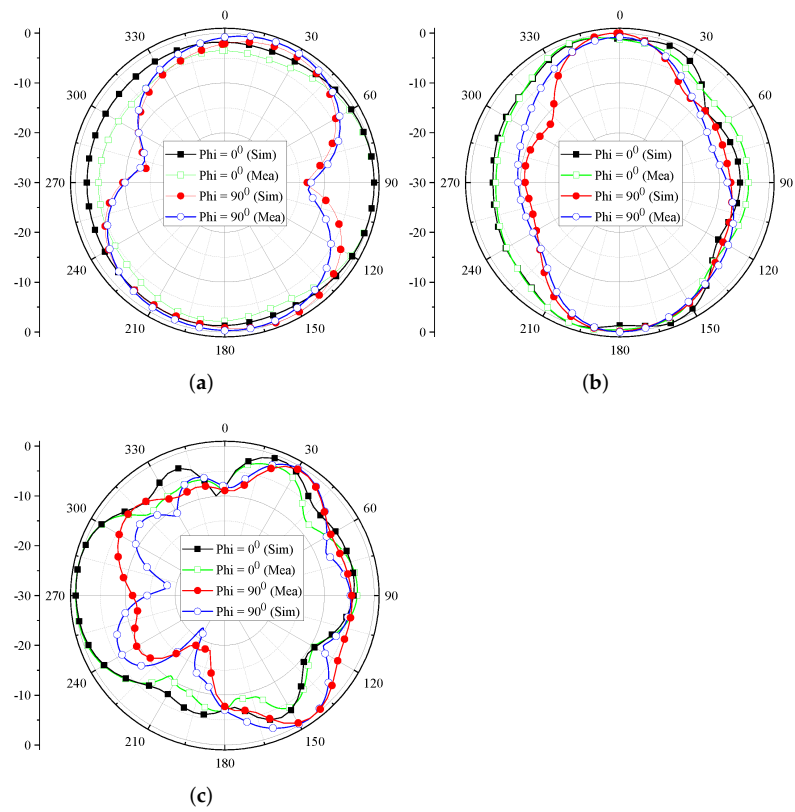
Figure 10. Radiation characteristics of the proposed UWB MIMO for port-1. (**a**) 3 GHz. (**b**) 6 GHz. (**c**) 9 GHz.
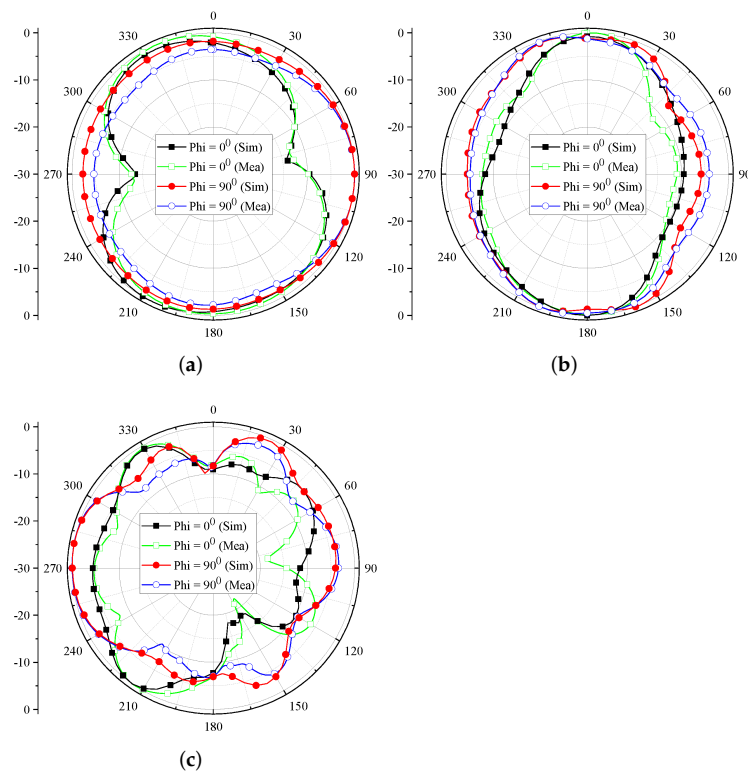
Figure 11. Radiation characteristics of the proposed UWB MIMO for port-2. (**a**) 3 GHz, (**b**) 6 GHz. (**c**) 9 GHz.
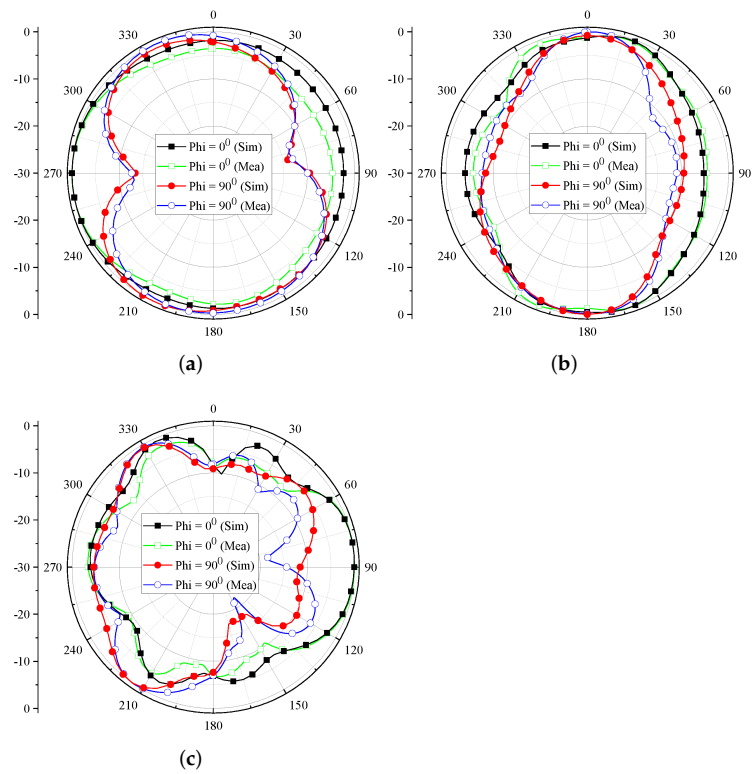
Figure 12. Radiation characteristics of the proposed UWB MIMO for port-3. (**a**) 3 GHz. (**b**) 6 GHz. (**c**) 9 GHz.
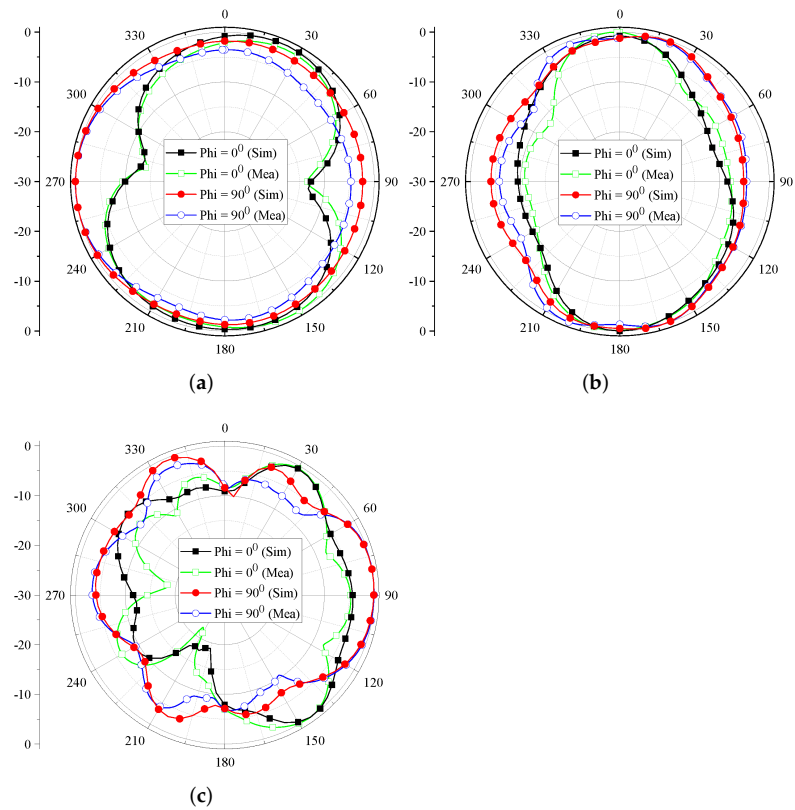
Figure 13. Radiation characteristics of the proposed UWB MIMO for port-4. (**a**) 3 GHz. (**b**) 6 GHz. (**c**) 9 GHz.

4. Diversity Performance Parameters

4.1. Envelope Correlation Coefficient (ECC)

To evaluate the proposed MIMO antenna's diversity performance, ECC is analyzed and presented in Figure 14. The far-field characteristics are used to determine the ECC as [27,28]:

$$ECC = \left| \frac{\iint_{4\pi} S_i(\theta,\phi).S_j^*(\theta,\phi)d\Omega}{\sqrt{\iint_{4\pi} S_i(\theta,\phi).S_i^*(\theta,\phi)d\Omega \iint_{4\pi} S_j(\theta,\phi).S_j^*(\theta,\phi)d\Omega}} \right|^2 \tag{1}$$

where S_i and S_j represents far-field radiation characteristics of port *i* and port *j*.

According to [29], the value of ECC should be set at <0.5 for practical applications. As shown in Figure 14, the proposed MIMO antenna exhibits ECC < 0.1.
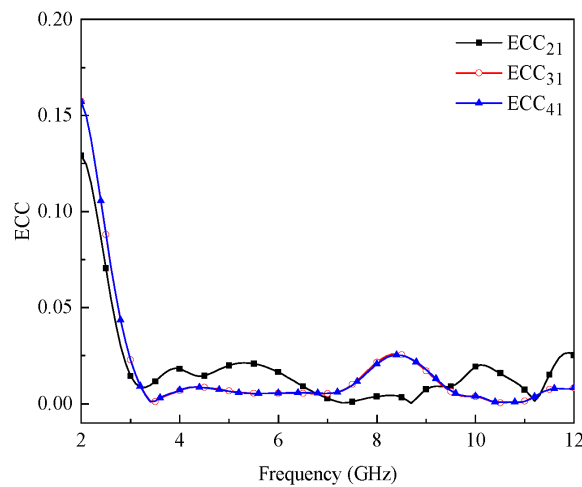
Figure 14. ECC of the proposed UWB MIMO antenna.

4.2. Diversity Gain (DG)

Another important feature that needs to be assessed is DG. The DG of the MIMO antennas should be high ($\approx$10 dB) in the operating bandwidth. It is expressed in terms of ECC as [28]:

$$DG = 10\sqrt{1 - ECC^2} \tag{2}$$

Figure 15 depicts the DG of the proposed MIMO antenna, and it is observed that it fluctuates around a 10 dB scale for the entire operating bandwidth.
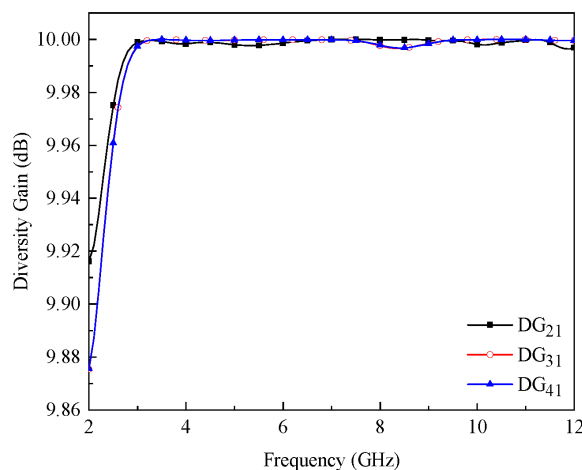
Figure 15. Diversity gain of the proposed UWB MIMO antenna.

4.3. Mean Effective Gain (MEG)

In comparison to an isotropic antenna, MEG is a measurement of how much power the antenna elements receive. The S-parameters of the MIMO antenna system can be used to calculate the MEG as [22,28]:

$$MEG_i = 0.5\left[1 - |S_{nn}|^2 - |S_{nm}|^2\right] \tag{3}$$

and

$$MEG_j = 0.5\left[1 - |S_{nm}|^2 - |S_{mm}|^2\right] \tag{4}$$

For the proposed MIMO antenna, the MEG is predicted between port-1 & port-2 and port-1 & port-3 (see Figure 16). It can be noted that the MEG of the ports is ≤ -3 dB, while the ratios of MEG1/MEG2 and MEG1/MEG3 are less than 3 dB.
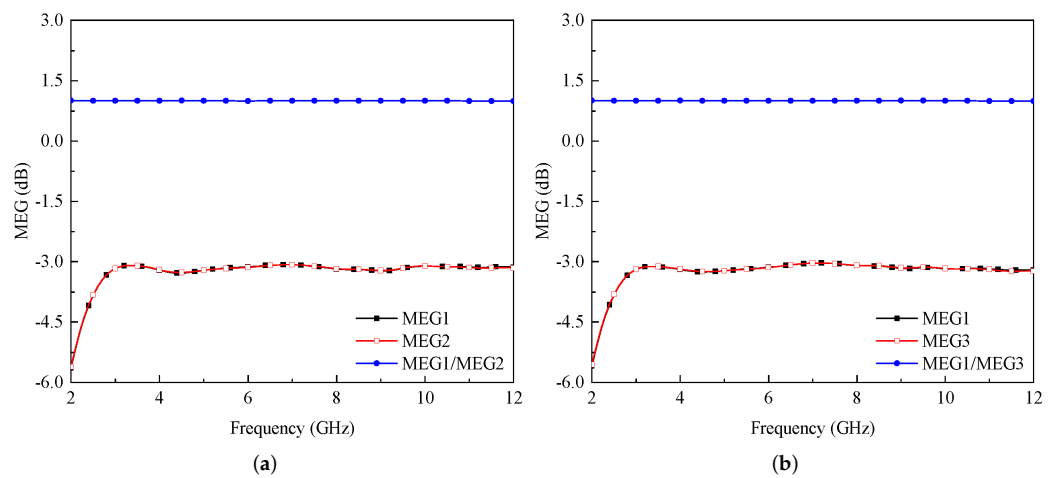
Figure 16. MEG between (**a**) port-1 & port-2 and (**b**) port-1 & port-3.

A comparison among proposed and previously presented four-port UWB MIMO antenna designs is presented in Table 1. The proposed design offers high impedance bandwidth compared to the designs presented in [8,12,13,19]. Although the dimensions of the proposed MIMO antenna are large, it provides comparable isolation and ECC characteristics without the utilization of any isolation enhancement network compared to the designs listed in Table 1. Moreover, the design of [18] did not utilize any isolation enhancement network, so it offers a high value of ECC compared to the proposed design. In addition, the authors in [8,13,14,16,19] calculated ECC using S-parameters, which is not recommended for practical applications.

Table 1. Comparison among proposed and previously published four-port UWB MIMO antennas.

Ref.	Array Size (mm^2)	Isolation Enhancement Network	Frequency Band (GHz)	Bandwidth (GHz)	Isolation (dB)	ECC	DG (dB)
[8]	32 × 36	FSS	3–10	7	>16	<0.0025	–
[12]	45 × 45	FSS + Decoupling Structure	3.1-10.6	7.5	>10	<0.17	>9.92
[13]	43 × 40	Decoupling Structure	3–11	8	>15	<0.2	>9.75
[14]	72 × 72	Neutralization Lines	2.8–13.3	10.5	>18	< 0.06	–
[16]	58 × 58	Decoupling Structure	3–16	13	>18	<0.07	–
[18]	40 × 40	Not utilized	3–13.5	10.5	>15	<0.4	>9.9
[19]	92 × 92	Neutralization Lines	2.84–11	8.16	>15	<0.02	–
This work	90 × 90	Not utilized	2.77–12	9.23	>15	<0.1	>9.97

5. Conclusions

A four-port MIMO antenna is designed for UWB applications. The array's single element consists of a fractal circular ring patch radiator backed by a square notch loaded trapezidal-shaped partial ground plane. The results show that the designed single antenna element resonates from 2.67 GHz to over 12 GHz, and it offers a peak realized gain of 5 dBi and an antenna efficiency of >75%. Furthermore, a novel MIMO antenna configuration is designed to assess single element performance for UWB MIMO applications. To achieve pattern and polarization diversity, the MIMO antenna elements are placed in a plus-shaped configuration. According to the measured data, the designed MIMO antenna operates in the frequency range of 2.77–12 GHz and has a 9.23 GHz impedance bandwidth. In addition, isolation of >15 dB is noted between antenna elements with an ECC of <0.1, DG of ≈10 dB, and MEG of <3 dB.

Author Contributions: Conceptualization, A.G.A., U.R. and S.M.A.; methodology, U.R., S.M.A., E.M.A. and M.A.; software, U.R.; validation, A.G.A., U.R., S.U., S.K. and S.M.A.; formal analysis, A.G.A., U.R., S.M.A., M.A. and M.D.; investigation, A.G.A., S.M.A., E.M.A., M.D.; resources, S.K., E.M.A., M.A. and M.D.; writing—original draft preparation, U.R.; writing–review and editing, S.U., S.K., S.M.A., M.A. and M.D.; visualization, U.R.; supervision, S.M.A. and M.A.; project administration, A.G.A., S.K. and E.M.A.; funding acquisition, S.U., E.M.A., M.A. and M.D. All authors have read and agreed to the published version of the manuscript.

Institutional Review Board Statement: Not applicable.

Informed Consent Statement: Not applicable.

Data Availability Statement: Not applicable.

Conflicts of Interest: The authors declare no conflict of interest.

References

1. Lim, E.G.; Wang, Z.; Lei, C.U.; Wang, Y.; Man, K. Ultra wideband antennas: Past and present. *IAENG Int. J. Comput. Sci.* **2010**, *37*, 1–11.
2. Abbas, S.; Desai, S.; Esselle, K.; Volakis, J.; Hashmi, R. Design and characterization of a flexible wideband antenna using polydimethylsiloxane composite substrate. *Int. J. Antennas Propag.* **2018**, *2018*, 4095765. [CrossRef]
3. Khan, M.S.; Capobianco, A.D.; Asif, S.M.; Anagnostou, D.E.; Shubair, R.M.; Braaten, B.D. A compact CSRR-enabled UWB diversity antenna. *IEEE Antennas Wirel. Propag. Lett.* **2016**, *16*, 808–812. [CrossRef]
4. Chandel, R.; Gautam, A.K.; Rambabu, K. Tapered fed compact UWB MIMO-diversity antenna with dual band-notched characteristics. *IEEE Trans. Antennas Propag.* **2018**, *66*, 1677–1684. [CrossRef]
5. Bahmanzadeh, F.; Mohajeri, F. Simulation and fabrication of a high-isolation very compact MIMO antenna for ultra-wide band applications with dual band-notched characteristics. *AEU-Int. J. Electron. Commun.* **2021**, *128*, 153505. [CrossRef]
6. Chandel, R.; Gautam, A.K.; Rambabu, K. Design and packaging of an eye-shaped multiple-input–multiple-output antenna with high isolation for wireless UWB applications. *IEEE Trans. Components Packag. Manuf. Technol.* **2018**, *8*, 635–642. [CrossRef]
7. Dey, A.B.; Pattanayak, S.S.; Mitra, D.; Arif, W. Investigation and design of enhanced decoupled UWB MIMO antenna for wearable applications. *Microw. Opt. Technol. Lett.* **2020**, *63*, 845–861. [CrossRef]
8. Bilal, M.; Saleem, R.; Abbasi, H.H.; Shafique, M.F.; Brown, A.K. An FSS-based nonplanar quad-element UWB-MIMO antenna system. *IEEE Antennas Wirel. Propag. Lett.* **2016**, *16*, 987–990. [CrossRef]
9. Naidu, P.R.T.; Saha, C.; Krishna, K.V.; Shaik, L.A.; Siddiqui, J.Y.; Antar, Y. Compact multiple EBG cells loaded UWB-narrowband antenna pair with high isolation for cognitive radio (CR) based MIMO applications. *AEU-Int. J. Electron. Commun.* **2020**, *127*, 153420. [CrossRef]
10. Kumar, N.; Kiran, K.U. Meander-line electromagnetic bandgap structure for UWB MIMO antenna mutual coupling reduction in E-plane. *AEU-Int. J. Electron. Commun.* **2020**, *127*, 153423. [CrossRef]
11. Modak, S.; Khan, T. A slotted UWB-MIMO antenna with quadruple band-notch characteristics using mushroom EBG structure. *AEU-Int. J. Electron. Commun.* **2021**, *134*, 153673. [CrossRef]

12. Bilal, M.; Shahid, S.; Khan, Y.; Rauf, Z.; Wagan, R.A.; Butt, M.A.; Khonina, S.N.; Kazanskiy, N.L. A Miniaturized FSS-Based Eight-Element MIMO Antenna Array for Off/On-Body WBAN Telemetry Applications. *Electronics* **2022**, *11*, 522. [CrossRef]

13. Amin, F.; Saleem, R.; Shabbir, T.; Rehman, S.U.; Bilal, M.; Shafique, M.F. A compact quad-element UWB-MIMO antenna system with parasitic decoupling mechanism. *Appl. Sci.* **2019**, *9*, 2371. [CrossRef]

14. Kumar, S.; Lee, G.H.; Kim, D.H.; Mohyuddin, W.; Choi, H.C.; Kim, K.W. Multiple-input-multiple-output/diversity antenna with dual band-notched characteristics for ultra-wideband applications. *Microw. Opt. Technol. Lett.* **2020**, *62*, 336–345. [CrossRef]

15. Ramanujam, P.; Venkatesan, P.R.; Arumugam, C.; Ponnusamy, M. Design of miniaturized super wideband printed monopole antenna operating from 0.7 to 18.5 GHz. *AEU-Int. J. Electron. Commun.* **2020**, *123*, 153273. [CrossRef]

16. Kumar, P.; Urooj, S.; Alrowais, F. Design and implementation of quad-port MIMO antenna with dual-band elimination characteristics for ultra-wideband applications. *Appl. Sci.* **2020**, *10*, 1715. [CrossRef]

17. Kumar, P.; Urooj, S.; Malibari, A. Design of quad-port ultra-wideband multiple-input-multiple-output antenna with wide axial-ratio bandwidth. *Sensors* **2020**, *20*, 1174. [CrossRef]

18. Khan, A.A.; Naqvi, S.A.; Khan, M.S.; Ijaz, B. Quad port miniaturized MIMO antenna for UWB 11 GHz and 13 GHz frequency bands. *AEU-Int. J. Electron. Commun.* **2021**, *131*, 153618. [CrossRef]

19. Addepalli, T.; Desai, A.; Elfergani, I.; Anveshkumar, N.; Kulkarni, J.; Zebiri, C.; Rodriguez, J.; Abd-Alhameed, R. 8-Port semi-circular arc MIMO antenna with an inverted L-strip loaded connected ground for UWB applications. *Electronics* **2021**, *10*, 1476. [CrossRef]

20. Sohi, A.K.; Kaur, A. A complementary Sierpinski gasket fractal antenna array integrated with a complementary Archimedean defected ground structure for portable 4G/5G UWB MIMO communication devices. *Microw. Opt. Technol. Lett.* **2020**, *62*, 2595–2605. [CrossRef]

21. Wang, E.; Wang, W.; Tan, X.; Wu, Y.; Gao, J.; Liu, Y. A UWB MIMO slot antenna using defected ground structures for high isolation. *Int. J. RF Microw.-Comput.-Aided Eng.* **2020**, *30*, e22155. [CrossRef]

22. Saadh, A.M.; Ashwath, K.; Ramaswamy, P.; Ali, T.; Anguera, J. A uniquely shaped MIMO antenna on FR4 material to enhance isolation and bandwidth for wireless applications. *AEU-Int. J. Electron. Commun.* **2020**, *123*, 153316. [CrossRef]

23. Anguera, J.; Andújar, A.; Jayasinghe, J.; Chakravarthy, V.; Chowdary, P.; Pijoan, J.L.; Ali, T.; Cattani, C. Fractal antennas: An historical perspective. *Fractal Fract.* **2020**, *4*, 3. [CrossRef]

24. Ray, K.P. Design aspects of printed monopole antennas for ultra-wide band applications. *Int. J. Antennas Propag.* **2008**, *2008*, 713858. [CrossRef]

25. Balanis, C.A. *Antenna Theory: Analysis and Design*; John Wiley & Sons: Hoboken, NJ, USA, 2015.

26. Rafique, U.; Ahmed, M.M.; Hassan, M.M.; Khalil, H. A modified super-wideband planar elliptical monopole antenna. In Proceedings of the 2018 Progress in Electromagnetics Research Symposium (PIERS-Toyama), Toyama, Japan, 1–4 August 2018; pp. 2344–2349.

27. Rafique, U.; Agarwal, S.; Nauman, N.; Khalil, H.; Ullah, K. Inset-fed Planar Antenna Array for Dual-band 5G MIMO Applications. *Prog. Electromagn. Res. C* **2021**, *112*, 83–98. [CrossRef]

28. Agarwal, S.; Rafique, U.; Ullah, R.; Ullah, S.; Khan, S.; Donelli, M. Double Overt-Leaf Shaped CPW-Fed Four Port UWB MIMO Antenna. *Electronics* **2021**, *10*, 3140. [CrossRef]

29. Koohestani, M.; Moreira, A.A.; Skrivervik, A.K. A novel compact CPW-fed polarization diversity ultrawideband antenna. *IEEE Antennas Wirel. Propag. Lett.* **2014**, *13*, 563–566. [CrossRef]